Doping-induced ferroelectric phase transition in strontium titanate: Observation of birefringence and coherent phonons under ultraviolet illumination

Y. Koyama,[1] T. Moriyasu,[1] E. Okamura,[1] Y. Yamada,[2] K. Tanaka,[3] and T. Kohmoto[1]
[1]*Graduate School of Science, Kobe University, Kobe 657-8501, Japan*
[2]*Institute for Chemical Research, Kyoto University, Kyoto 611-0011, Japan*
[3]*Graduate School of Science, Kyoto University, Kyoto 606-8502, Japan*
(Received 14 October 2008; revised manuscript received 21 September 2009; published 14 January 2010)

The doping-induced ferroelectric phase transition in Ca-doped $SrTiO_3$ is investigated by observing the birefringence and coherent phonons. The structural phase-transition temperature is determined by the birefringence measurement. Coherent phonons of the soft modes are studied by using ultrafast polarization spectroscopy. Two phonon modes are observed to be softened toward the ferroelectric phase-transition point at 28 K and other two phonon modes are observed to be softened toward the structural phase-transition point at 180 K. Another structural deformation at 25 K is found below the ferroelectric phase-transition temperature. From the temperature dependence of phonon frequencies under an ultraviolet (UV) illumination, a shift of the ferroelectric phase-transition point toward the lower temperature side is found. A decrease in phonon frequencies after the UV illumination is also found.

DOI: 10.1103/PhysRevB.81.024104 PACS number(s): 77.84.Ek, 77.80.B-, 78.20.Fm, 63.20.dd

I. INTRODUCTION

There has been significant interest in a quantum paraelectric material strontium titanate ($SrTiO_3$), and its lattice dynamics and unusual dielectric character have been extensively studied. $SrTiO_3$ (STO) is known to undergo a structural phase transition at $T_c=105$ K.[1] The cubic (O_h) structure above T_c, where all phonon modes are Raman forbidden, changes into the tetragonal (D_{4h}) structure below T_c, where Raman-allowed modes of symmetries A_{1g} and E_g appear.[2] In low temperatures, its dielectric constant increases up to about 30 000. The dielectric constant increases extraordinarily with decreasing temperature while the paraelectric phase is stabilized by quantum fluctuations without any ferroelectric phase transition even below the classical Curie temperature $T_c=37$ K.[3] In $SrTiO_3$, a ferroelectric transition is easily induced by a weak perturbation such as an uniaxial stress,[4] an isotopic substitution of oxygen 18 for oxygen 16,[5] and an impurity doping.[6,7]

According to the measurement of dielectric constants, $Sr_{1-x}Ca_xTiO_3$ undergoes a ferroelectric transition above the critical Ca concentration $x_c=0.0018$, where doped Ca ions are substituted for the Sr ions.[8–10] The cubic structure above the structural phase-transition temperature T_{c1} changes into the tetragonal structure below T_{c1} and into the rhombohedral structure below the ferroelectric transition temperature T_{c2}. The structural phase transition at T_{c1} is also antiferrodistortive as in pure $SrTiO_3$ at 105 K.[8] The temperature of the structural phase transition is $T_{c1}=180$ K and that of the ferroelectric transition is $T_{c2}=28$ K for $x=0.011$.[11] As in the case of impurity systems, Li-doped $KTaO_3$ and Nb-doped $KTaO_3$,[6] off-centered impurity ions are supposed. Their polarized dipole moments show a ferroelectric instability below the ferroelectric transition temperature.[6] In the case of Ca-doped $SrTiO_3$ (SCTO), a spontaneous polarization occurs along [110] directions in the c plane, where the tetragonal (D_{4h}) symmetry is lowered to C_{2v}.[8] With decreasing temperature a ferroelectric ordering process dominates, that is, due to the thermal growth of the polarization clouds surrounding the off-center Ca^{2+} dipoles.[8] The system behaves like a superparaelectric as the ferroelectric nano-ordered regions contain disordered clusterlike regions. The investigation by x-ray and neutron diffractions and first-principles calculations[12] suggests that polar instabilities originating from the off-center displacements of Ca^{2+} ions are not likely to directly polarize the host matrix by an electrostatic mechanism. Instead, the possible role of random fields in inducing the presence of disordered polar clusters was suggested, which is similar to polar nanoregions in relaxor materials.

Recently, a gigantic change in the dielectric constant by an ultraviolet (UV) illumination was discovered,[13,14] and a deeper interest has been taken in $SrTiO_3$ again. The origin of the giant dielectric constants, however, has not yet been clarified. In Ca-doped $SrTiO_3$, it was reported that a UV illumination causes a ferroelectric peak shift of the dielectric constant toward the lower temperature side.[11] In several ferroelectric materials such as $BaTiO_3$,[15] SbSI,[16] and oxygen-isotope-substituted $SrTiO_3$,[17] the T_c reduction under a UV illumination has been observed.

The optical information on the dielectric response is usually obtained from the experiments of Raman scattering or infrared spectroscopy. The usefulness of the investigation of low-frequency dielectric response by observing coherent phonons have also been demonstrated by the time-resolved study of the dynamics of phonons[18] and phonon polaritons.[19] At low frequencies this technique is very sensitive and provides a very good signal-to-noise ratio as compared to the conventional frequency-domain techniques while at higher frequencies a better performance will be achieved by using the conventional techniques. Therefore the coherent phonon spectroscopy and the conventional frequency-domain techniques can be considered to be complementary methods for the investigation of the dielectric response. Under a UV illumination, $SrTiO_3$ and Ca-doped $SrTiO_3$ show a broadband luminescence in the visible region originated from a relaxed excited state.[20] The coherent phonon spectroscopy is not sen-

 ©2010 The American Physical Society

sitive to the luminescence and a powerful technique to investigate UV-illumination effects in paraelectric materials as compared to the Raman-scattering measurement because in Raman-scattering experiments, it is not easy to separate Raman-scattering signals from the luminescence.

In the present study, the doping-induced ferroelectric phase transition in Ca-doped $SrTiO_3$ is investigated by observing the birefringence and coherent phonons. In the birefringence measurement, the structural and the ferroelectric phase-transition temperatures are examined. Coherent phonons are observed by using ultrafast polarization spectroscopy with the pump-probe technique. The soft phonon modes related to the structural and the ferroelectric phase transitions are studied, and their frequencies are obtained from the observed coherent phonon signals. The behavior of the softening toward each phase-transition temperature and the UV-illumination effect on the ferroelectric transition are discussed. In addition to the ferroelectric phase transition at 28 K, another structural deformation at 25 K is found. A shift of the ferroelectric phase-transition temperature under the UV illumination and a decrease in the phonon frequencies after the UV illumination are found. We show the approach in the time domain is very useful for the study of the soft phonon modes and their UV-illumination effect in dielectric materials.

II. EXPERIMENT

The experiments are performed on a single crystal of Ca-doped $SrTiO_3$ with the Ca concentration of $x=0.011$, which was grown by the floating-zone method. The value of x was determined by the empirical relation of Bednorz and Müller.[7] The thickness of the sample is 0.5 mm. A dc electric field, whose voltage is 300 V, is applied between two Au electrodes. The electrodes with a gap of 0.8 mm are deposited on a (100) surface of the sample by sputtering. The direction of the dc electric field is parallel to the [100] direction of the crystal.

A. Birefringence measurement

The structural phase-transition $(O_h \rightarrow D_{4h})$ temperature, $T_{c1}=180$ K, is obtained from the temperature dependence of the birefringence. The ferroelectric phase-transition temperature, $T_{c2}=28$ K, was determined by the measurement of dielectric constants.[11] The change in birefringence is detected as the change in the polarization of a linearly polarized probe light provided by a Nd:YAG laser (532 nm).

B. Observation of coherent phonons

Coherent phonons are observed by ultrafast polarization spectroscopy with the pump-probe technique. Coherent phonons are created by femtosecond optical pulses through the process of impulsive stimulated Raman scattering, and are detected by monitoring the time-dependent anisotropy of refractive index induced by the pump pulse. The pump pulse is provided by a Ti:sapphire regenerative amplifier whose wavelength, pulse energy, and pulse width at the sample are 790 nm, 2 μJ, and 0.2 ps, respectively. The probe pulse is provided by an optical parametric amplifier whose wavelength, pulse energy, and pulse width are 690 nm, 0.1 μJ, and 0.2 ps, respectively. The repetition rate of the pulses is 1 kHz. The linearly polarized pump and probe beams are nearly collinear and perpendicular to the (001) surface of the sample, and are focused on the sample in a temperature-controlled refrigerator. The waist size of the beams at the sample is about 0.5 mm.

The induced anisotropy of refractive index is detected by a polarimeter[21,22] with a quarter-wave plate as the polarization change in the probe pulse. The plane of polarization of the probe pulse is tilted by 45° from that of the pump pulse. The two different wavelengths for the pump and probe pulses and pump-cut filters are used to eliminate the leak of the pump light from the input of the polarimeter. The time evolution of the signal is observed by changing the optical delay between the pump and probe pulses. The pump pulse is switched on and off shot by shot by using a photoelastic modulator, a quarter-wave plate, and a polarizer, and the output from the polarimeter is lock-in detected to improve the signal-to-noise ratio.

The source of UV illumination is provided by the second harmonics (380 nm, 3.3 eV) of the output from another mode-locked Ti:sapphire laser, whose energy is larger than the optical band gap of $SrTiO_3$ (3.2 eV). Since the repetition rate of the UV pulses is 80 MHz, this UV illumination can be considered to be continuous in the present experiment, where the UV-illumination effect appearing more than one minute after is studied. The UV beam is illuminated on the 0.8 mm gap between the two electrodes.

III. RESULTS

A. Birefringence measurement

Figure 1 shows the temperature dependences of the change in birefringence in STO and SCTO between 4.5 and 250 K, where the dc electric field and the UV illumination are off, and the polarization plane of the probe light is along the [110] and [100] axes. In $SrTiO_3$, a change in birefringence appears below $T_c=105$ K, which is the temperature of the structural phase transition, and is increased as the temperature is decreased. In Ca-doped $SrTiO_3$, large changes in birefringence come out at $T_{c1}=180$ K, which is the temperature of the structural phase transition, and at $T_{c2}=28$ K, which is the temperature of the ferroelectric phase transition. The change in birefringence is increased as the temperature is decreased from T_{c1} to T_{c2}, as well as the case in $SrTiO_3$, and shows a increase in the gradient for both axes around T_{c2}. Below T_{c2}, another kind of lattice distortion is added, and the peaks of Δn due to the competition between the two kinds of lattice distortion appear. In both $SrTiO_3$ and Ca-doped $SrTiO_3$, a cusp on the birefringence curve appears around $T_c=105$ K and $T_{c1}=180$ K, respectively, because of the fluctuation associated with the second-order structural phase transition.[23]

B. Observation of coherent phonons

The angular dependence of the coherent phonon signal in Ca-doped $SrTiO_3$ at 50 K is shown in Fig. 2(a), where the

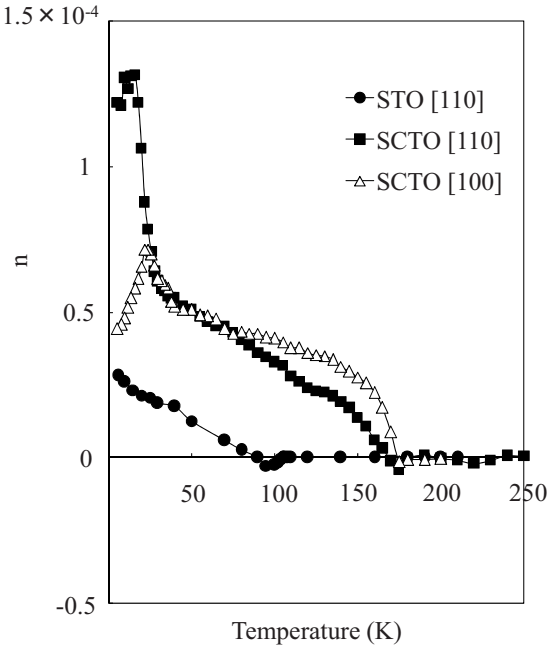

FIG. 1. Temperature dependences of the change in birefringence between 4.5 and 250 K in $SrTiO_3$ and Ca-doped $SrTiO_3$. The polarization plane of the probe light for $SrTiO_3$ is along the [110] axis (STO [110], solid circles). That for Ca-doped $SrTiO_3$ is along the [110] axis (SCTO [110], solid squares) and along the [100] axis (SCTO [100], open triangles).

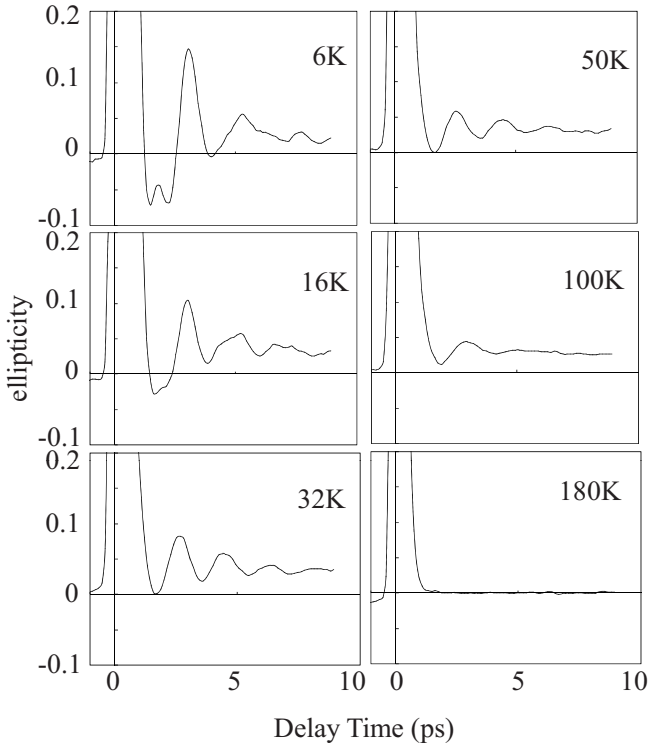

FIG. 3. Temperature dependence of the coherent phonon signal in Ca-doped $SrTiO_3$ observed for the 45° pumping.

angle between the [100] axis of the crystal and the polarization plane of the pump pulse is 0°, 25°, and 45°. The angle between the polarization planes of the pump and probe pulses is fixed to 45°. Vertical axis is the ellipticity in electric field amplitude of the transmitted probe. At zero delay, a large signal due to the optical Kerr effect, whose width is determined by the laser-pulse width, appears. After that, a damped oscillation of coherent phonons is observed. For the 0° pumping a 0.5 ps period signal appears while it disappears for the 45° pumping and a 2 ps period signal appears. The Fourier transform of the coherent phonon signals in Fig. 2(a) is shown in Fig. 2(b). The oscillation frequency of the signal for the 0° pumping is 1.9 THz and that for the 45° pumping is 0.5 THz. For other pumping angles both frequency components coexist in the coherent phonon signal. These phonon modes are the soft modes related to the structural phase transition at $T_{c1}=180$ K. From the oscillation frequencies the 1.9 THz component corresponds to the A_{1g} mode, and the 0.5 THz components to the E_g mode, which are assigned from the modes of pure $SrTiO_3$ (Ref. 2) and from that of $Sr_{1-x}Ca_xTiO_3$ ($x=0.007$).[8]

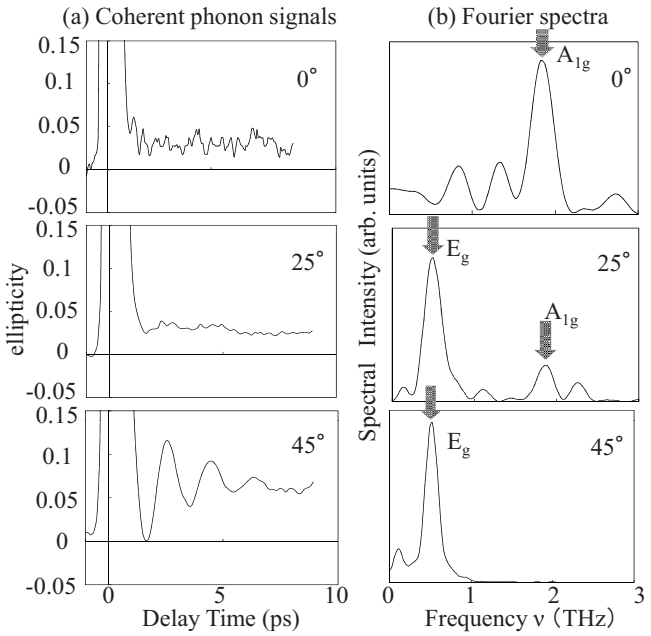

FIG. 2. (a) Coherent phonon signals in Ca-doped $SrTiO_3$ at 50 K observed for the 0°, 25°, and 45° pumping, where the angle between the [100] axis of the crystal and the polarization direction of the pump pulse is changed. (b) Fourier transform of the coherent phonon signals in (a).

The temperature dependence of the coherent phonon signal for the 45° pumping, which corresponds to the E_g mode, is shown in Fig. 3. At 6 K some oscillation components, which have different frequencies, are superposed. As the temperature is increased, the number of the oscillation components is decreased, the oscillation period becomes longer and the relaxation time becomes shorter. At $T_{c1}=180$ K, which is the structural phase-transition temperature obtained from the birefringence measurement, no signal of coherent phonons is observed.

The temperature dependence of the coherent phonon signal observed for the 25° pumping are shown in Figs. 4 and 5. Figure 4(a) shows the coherent phonon signals below the ferroelectric phase-transition temperature T_{c2} and Fig. 5(a)

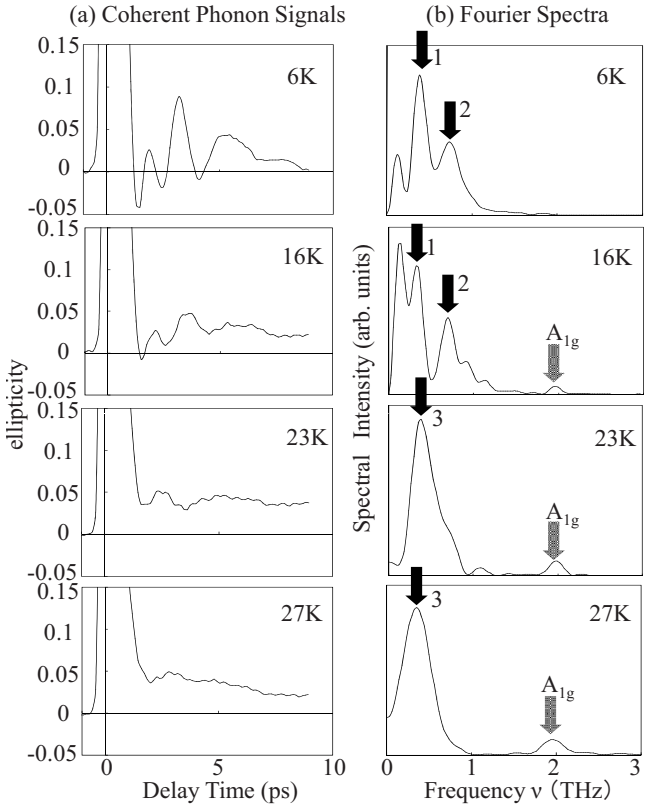

FIG. 4. (a) Temperature dependence of the coherent phonon signal in Ca-doped $SrTiO_3$ observed for the 25° pumping below the ferroelectric phase-transition temperature T_{c2}. (b) Fourier transform of the coherent phonon signals in (a).

shows those above T_{c2}. Figure 4(b) shows the Fourier transform of the coherent phonon signals in Fig. 4(a), where the peaks with arrows 1, 2, and 3 correspond to the ferroelectric phonon modes.[8] Figure 5(b) shows the Fourier transform of the coherent phonon signals in Fig. 5(a), where modes 1, 2, and 3 disappear but the A_{1g} and E_g modes related to the structural phase-transition remain.

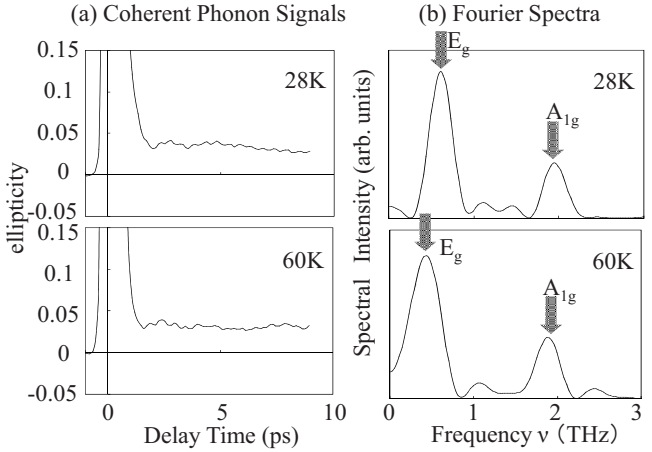

FIG. 5. (a) Temperature dependence of the coherent phonon signal in Ca-doped $SrTiO_3$ observed for the 25° pumping above the ferroelectric phase-transition temperature T_{c2}. (b) Fourier transform of the coherent phonon signals in (a).

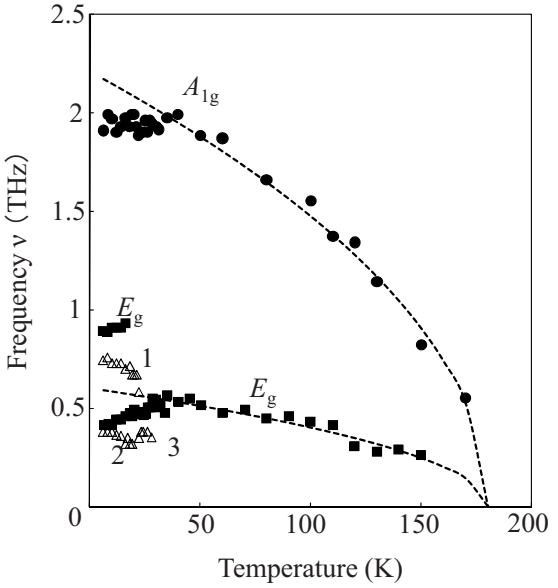

FIG. 6. Temperature dependence of the phonon frequencies obtained from the coherent phonon signals below T_{c1}. The solid circles are the oscillation frequency for the A_{1g} mode and the solid squares are that for the E_g mode. The broken curves describe a temperature dependence of the form $\omega \propto (T_c - T)^n$, where $T_c = 180$ K and $n = 0.5$ for both modes. The open triangles are that for modes 1, 2, and 3 related to the ferroelectric phase transition.

IV. DISCUSSION

A. Phonon frequencies

Each component of the coherent phonon signal is expressed well by a damped oscillation $Ae^{-\gamma t} \sin \omega t$, where ω is an oscillation frequency and γ is a relaxation rate. This sine-type function is expected for phonons induced by impulsive stimulated Raman scattering.[24,25] The temperature dependence of the oscillation frequencies obtained from the observed coherent phonon signals below T_{c1} is shown in Fig. 6. The solid circles are the oscillation frequency for the A_{1g} mode and the solid squares are that for the E_g mode. The open triangles are that for modes 1, 2, and 3 which are related to the ferroelectric phase transition. As for the A_{1g} and E_g modes, as the temperature is increased from 6 K, the oscillation frequencies decrease and approach to zero at the structural phase-transition temperature T_{c1} for both modes. This result is consistent with the temperature dependence of phonon frequency observed by Raman scattering[2] and coherent phonons[26] for pure $SrTiO_3$ except for the phase-transition temperature. The broken curves describe a temperature dependence of the form $\omega \propto (T_c - T)^n$. The experimental results for the temperature region between T_{c1} and T_{c2} are explained well by $n = 0.5$ for both modes. Below the ferroelectric phase-transition temperature T_{c2}, another mode appears at 0.9 THz. It is considered that the doubly degenerate E_g mode is split into two components under the tetragonal-to-rhombohedral lattice distortion.

The temperature dependence of the phonon frequencies, which are related to the ferroelectric phase transition, obtained from the observed coherent phonon signals below T_{c2}

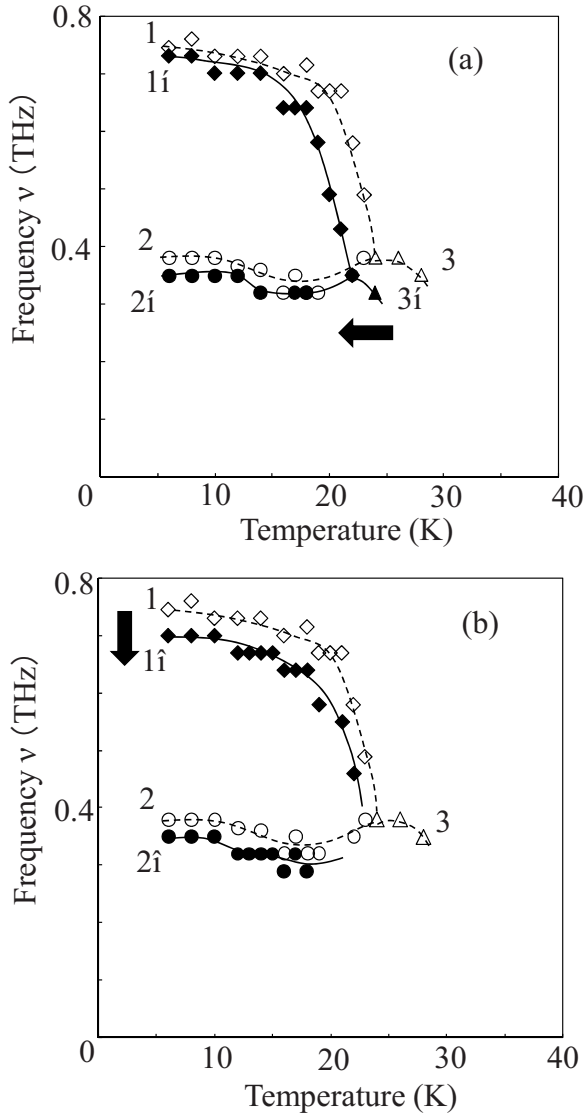

FIG. 7. Temperature dependence of the phonon frequencies (a) under dark (1, 2, 3) and under UV (1′,2′,3′) illumination below T_{c2}, which correspond the phonon modes related to the ferroelectric phase transition, and (b) under dark (1, 2, 3) and after UV (1″,2″,3″) illumination, where the intensity of the UV illumination is 7 mW/mm^2.

is shown in Fig. 7(a), where only the frequencies of the reproducible peaks in the Fourier spectrum are plotted. While the lowest peaks at 6 and 16 K in Fig. 4, for example, may be the third mode observed in the Raman experiment,[8] the frequencies of the peaks with poor reproducibility are not plotted in Figs. 6 and 7. Under dark illumination, two phonon modes 1 and 2 are softened toward about 25 K and degenerate into mode 3, which seems to be softened toward the ferroelectric phase-transition temperature T_{c2}=28 K. The lift of degeneracy for mode 3 below T_{c2} suggests that another structural deformation occurs at 25 K. In the Raman-scattering experiment,[8] three modes deriving from the TO_1 mode has been observed. The three modes do not all split off at the same temperature; the highest-energy component splits off at the ferroelectric transition temperature while the other two split off at the temperature about 3 K lower. These two temperatures may correspond to the two temperatures, 28 and 25 K, observed in our experiment, and the temperature differences are nearly equal to each other. The existence of the second structural deformation at 25 K is consistent with the Raman-scattering data.

B. UV-illumination effect

In order to examine the UV-illumination effect, two types of measurements, under the UV illumination and after the UV illumination, are carried out. The temperature dependence of the phonon frequencies under the UV illumination is shown in Fig. 7(a), where the intensity of the UV illumination is 7 mW/mm^2. As is seen in Fig. 7(a), the temperature, toward which the two modes 1 and 2 are softened and degenerate into mode 3, shifts to the lower temperature side. The temperature shift due to the UV-illumination effect is ~3 K.

Doped Ca ions behave as permanent dipoles and ferroelectric clusters are formed around Ca dipoles with high polarizability of the host crystal. The ferroelectric transition is caused by the ordering of randomly distributed Ca dipoles. The UV-illumination-induced T_c reduction is related to the screening of the internal macroscopic field by UV-excited carriers. Under the UV-illumination nonequilibrium carriers appear, which are captured by traps and screen the polarization field. The ordering is prevented by the photoexcited carriers. Thus, the screening effect due to the UV-excited carriers weaken the Coulomb interaction between dipoles, and the transition temperature is decreased.

The theoretical T_{c2} reduction under the UV illumination ΔT_{c2} is given by[11]

$$\frac{\Delta T_{c2}}{T_{c2}(0)} = 1 - \left(1 + \lambda a + \frac{\gamma}{4\pi}\lambda^2 a^2\right)\exp(-\lambda a), \qquad (1)$$

where $T_{c2}(0)$ is the transition temperature before the UV illumination, λ is the inverse of the screening length, a is the mean separation between the dipoles, and γ is the number of the nearest-neighbor dipoles. The expression of λ is presented by $\lambda = \sqrt{\frac{ne^2}{\varepsilon\varepsilon_0 kT}}$, where n is the carrier concentration which depends on the UV-illumination intensity and ε is the relative dielectric constant. In the present case, the domain is large enough and the dipole-dipole interaction is expressed as a simple Coulomb interaction. The UV-illumination-intensity dependence of the T_{c2} reduction for $Sr_{1-x}Ca_xTiO_3$ (x=0.011) was analyzed by using Eq. (1). Assuming that the carrier concentration is proportional to the UV-illumination intensity, the fitting result reproduced well the experimental result obtained in the measurement of dielectric constants.[11] Here we estimate the inverse λ of the screening length at the UV-illumination intensity of 7 mW/mm^2. As a result of the measurement of dielectric constant,[11] the carrier concentration is $n=2.5\times10^{17}$ cm^{-3} at 3 mW/mm^2. From this value we can estimate the carrier concentration to be $n=5.8\times10^{17}$ cm^{-3} at 7 mW/mm^2. The value of the inverse of the screening length is obtained as

$$\lambda = \sqrt{\frac{ne^2}{\varepsilon\varepsilon_0 kT}} = \sqrt{\frac{n8\pi a_B E_{1s}}{\varepsilon kT}} = 1.1 \times 10^7 \ (/\mathrm{cm}), \quad (2)$$

where a_B and E_{1s} are Bohr radius and the energy of the hydrogen atom in the $1s$ ground state, respectively, and we use the dielectric constant $\varepsilon=4$ in the visible region. Substituting the value of λ into Eq. (1), the shift of the transition temperature can be estimated to be $\Delta T_{c2} \sim 8$ K. This estimation is not inconsistent with the observed values of the temperature shift in the experiment of coherent phonons, in which the value of the observed transition temperature shift is ~ 3 K.

The temperature dependence of the phonon frequencies after the UV illumination is shown in Fig. 7(b), where the UV illumination of 7 $\mathrm{mW/mm^2}$ is on before the coherent phonon measurement but is off during the measurement. In this case, on the other hand, the shift of the softening temperature for modes 1 and 2 is not clear. The phonon frequencies for modes 1 and 2 are decreased while the coherent phonon signal for mode 3 is not observed. The relaxation time of the UV-illumination induced carriers is on the order of milliseconds below 30 K for $SrTiO_3$.[20] As is seen in Fig. 7(b), however, it is suggested that the UV-illumination effect, frequency decrease for modes 1 and 2 and disappearance of mode-3 signal, remains for at least several minutes, even if the UV illumination is switched off, although the T_c shifting effect disappears immediately.

V. SUMMARY

We observed the temperature dependences of the birefringence and the coherent phonon signal to investigate the doping-induced ferroelectric phase transition in Ca-doped $SrTiO_3$ with the Ca concentration of $x=0.011$. In the birefringence measurement, it was confirmed that the structural phase-transition temperature is $T_{c1}=180$ K. Coherent phonons were observed by using ultrafast polarization spectroscopy. The damped oscillations of coherent phonons for the A_{1g} and E_g modes, which contribute to the structural phase transition at $T_{c1}=180$ K, and for the modes 1, 2, and 3, which contribute to the ferroelectric phase transition at $T_{c2}=28$ K, were observed. The phonon frequencies were obtained from the observed signals of coherent phonons, and their softening toward each phase-transition temperature was observed. Another structural deformation at 25 K was found in addition to the ferroelectric phase transition at T_{c2}. It was found that the UV illumination causes the shift of the ferroelectric phase-transition point toward the lower temperature side, and the temperature shift is ~ 3 K. The decrease in the phonon frequencies after the UV illumination suggests the UV-illumination effect remains even if the UV illumination is switched off. It was shown that the coherent phonon spectroscopy in the time domain is a very useful approach to study the soft phonon modes and their UV-illumination effect in dielectric materials.

[1] J. F. Scott, Rev. Mod. Phys. **46**, 83 (1974), and references therein.
[2] P. A. Fleury, J. F. Scott, and J. M. Worlock, Phys. Rev. Lett. **21**, 16 (1968).
[3] K. A. Müller and H. Burkard, Phys. Rev. B **19**, 3593 (1979).
[4] H. Uwe and T. Sakudo, Phys. Rev. B **13**, 271 (1976).
[5] M. Itoh, R. Wang, Y. Inaguma, T. Yamaguchi, Y.-J. Shan, and T. Nakamura, Phys. Rev. Lett. **82**, 3540 (1999).
[6] B. E. Vugmeister and M. P. Glinchuk, Rev. Mod. Phys. **62**, 993 (1990).
[7] J. G. Bednorz and K. A. Müller, Phys. Rev. Lett. **52**, 2289 (1984).
[8] U. Bianchi, W. Kleemann, and J. G. Bednorz, J. Phys.: Condens. Matter **6**, 1229 (1994).
[9] U. Bianchi, J. Dec, W. Kleemann, and J. G. Bednorz, Phys. Rev. B **51**, 8737 (1995).
[10] A. Bürgel, W. Kleemann, and U. Bianchi, Phys. Rev. B **53**, 5222 (1995).
[11] Y. Yamada and K. Tanaka, J. Phys. Soc. Jpn. **77**, 5 (2008).
[12] G. Geneste and J.-M. Kiat, Phys. Rev. B **77**, 174101 (2008).
[13] M. Takesada, T. Yagi, M. Itoh, and S. Koshihara, J. Phys. Soc. Jpn. **72**, 37 (2003).
[14] T. Hasegawa, S. Mouri, Y. Yamada, and K. Tanaka, J. Phys. Soc. Jpn. **72**, 41 (2003).
[15] G. Godefroy, P. Jullien, and L. Cai, Ferroelectrics **13**, 309 (1976).
[16] S. Ueda, I. Tatsuzaki, and Y. Shindo, Phys. Rev. Lett. **18**, 453 (1967).
[17] Y. Yamada and K. Tanaka, J. Lumin. **112**, 259 (2005).
[18] T. P. Dougherty, G. P. Wiederrecht, K. A. Nelson, M. H. Garrett, H. P. Jensen, and C. Warde, Science **258**, 770 (1992).
[19] H. J. Bakker, S. Hunsche, and H. Kurz, Rev. Mod. Phys. **70**, 523 (1998).
[20] T. Hasegawa, M. Shirai, and K. Tanaka, J. Lumin. **87-89**, 1217 (2000).
[21] T. Kohmoto, Y. Fukuda, M. Kunitomo, and K. Isoda, Phys. Rev. B **62**, 579 (2000).
[22] R. V. Jones, Proc. R. Soc. London, Ser. A **349**, 423 (1976).
[23] E. Courtens, Phys. Rev. Lett. **29**, 1380 (1972).
[24] Y.-X. Yan, E. B. Gamble, Jr., and K. A. Nelson, J. Chem. Phys. **83**, 5391 (1985).
[25] G. A. Garrett, T. F. Albrecht, J. F. Whitaker, and R. Merlin, Phys. Rev. Lett. **77**, 3661 (1996).
[26] T. Kohmoto, K. Tada, T. Moriyasu, and Y. Fukuda, Phys. Rev. B **74**, 064303 (2006).